

Permittivity Measurements at Microwave Frequencies Using Epsilon-Near-Zero (ENZ) Tunnel Structure

Humberto Lobato-Morales, *Student Member, IEEE*, D. V. B. Murthy, Alonso Corona-Chávez, *Senior Member, IEEE*, José Luis Olvera-Cervantes, Juan Martínez-Brito, and Luis Gerardo Guerrero-Ojeda, *Member, IEEE*

Abstract—A planar epsilon-near-zero (ENZ) tunnel structure implemented on substrate integrated waveguide (SIW) technology is used to evaluate the complex dielectric permittivity of various materials. Design, optimization, and fabrication of the ENZ tunnel structure are explained. Simulations and measurements on various dielectric samples using the cavity perturbation technique of the proposed structure are presented. Measured values of the permittivity are in good agreement with standard values. Sensitivity analyses are performed on the ENZ structure and the conventional SIW cavity techniques. The proposed structure has very high sensitivity, which yields more accurate results when compared to other techniques, such as perturbation of conventional cavities.

Index Terms—Cavity perturbation methods, epsilon-near-zero (ENZ), permittivity measurements, substrate integrated waveguide (SIW).

I. INTRODUCTION

MICROWAVE engineering needs precise knowledge on electromagnetic properties of materials at microwave frequencies for various applications. Several methods for the evaluation of permittivity and permeability of materials at microwave frequencies are available. These methods are mainly based on waveguides and include reflection-transmission methods [1]–[3] and resonance techniques [4]. Microwave resonant cavities are often used for dielectric measurements due to their unique characteristics of high quality factor Q and good sensitivity [5]–[7]. However, compact devices are required for small measurement systems [8]. Bernard *et al.* performed dielectric permittivity measurements of materials by means of a microstrip ring resonator [6]. Nevertheless, microstrip structures suffer of low Q factors in the range of 50–100 [5], [9].

With the development of substrate integrated waveguide (SIW) technology, it is possible to design cavities in planar form [7]. Moreover, this technique provides low profile, low cost, and ease of fabrication of the structures. Lobato *et al.*

Manuscript received November 26, 2010; revised March 03, 2011; accepted March 04, 2011. Date of publication April 29, 2011; date of current version July 13, 2011.

H. Lobato-Morales, D. V. B. Murthy, A. Corona-Chávez, and J. L. Olvera-Cervantes are with the Emerging Microwave Technologies Group (EMT), Instituto Nacional de Astrofísica, Óptica y Electrónica (INAOE), Tonantzintla, Puebla 72840, México (e-mail: humbertolm@ieee.org).

J. Martínez-Brito and L. G. Guerrero-Ojeda are with the Computers, Electronics and Mechatronics Department, Universidad de las Américas-Puebla (UDLA-P), Cholula, Puebla 72810, México.

Color versions of one or more of the figures in this paper are available online at <http://ieeexplore.ieee.org>.

Digital Object Identifier 10.1109/TMTT.2011.2132141

performed the detailed analysis on the cavity perturbation technique of SIW cavity resonator for dielectric measurements [10]. A SIW cavity resonator is used to measure the dielectric properties of binary mixtures [7]. Recently, epsilon-near-zero (ENZ) metamaterial technology has received much attention because of its potential advantage in miniaturization and enhanced sensitivity, as energy can be tunneled through a narrow waveguide. This phenomenon has led to several potential applications [11]–[13]. In particular, this technology can be applied to the measurement of complex permittivity of the materials. Alu and Engheta [11] performed theoretical study of ENZ tunnels for the evaluation of complex permittivity of the materials. However, the proposed theory is not validated experimentally. In [14], the dielectric constant measurements using the ENZ tunnels are performed with SIW technology [15]; however, no analysis of the dielectric loss part is presented.

In this paper, a novel ENZ tunneling circuit using SIW technology is proposed to evaluate the real and imaginary parts of the dielectric permittivity of materials. Moreover, this device offers higher sensitivity when compared with conventional resonant techniques due to the high E -field concentration through the narrow tunnel [11]. This paper is organized as follows. Section II describes the design procedure, simulation results, and fabrication of the ENZ tunnel using SIW technology; a sensitivity analysis on tunnel structures is also performed. Section III presents the measurements and characterization of various dielectric samples using the proposed structure and cavity perturbation technique. Section IV presents the sensitivity characteristics of the ENZ tunnel structure and comparison by using resonant techniques.

II. DESIGN OF ENZ STRUCTURE WITH SIW TECHNOLOGY

A. Design of the ENZ Structure

The ENZ tunneling effect can be obtained inside a rectangular waveguide channel of narrow height that operates near the cutoff frequency of its dominant TE_{10} mode. The cutoff frequency (f_{c10}) of a rectangular waveguide in its dominant mode TE_{10} is obtained by

$$f_{c10} = \frac{c}{2b\sqrt{\epsilon_r}} \quad (1)$$

where c is the speed of light in a vacuum, b is the width of the waveguide, and ϵ_r is the relative real permittivity of the material filling the waveguide.

The tunneling effect can be realized by using waveguide technology. This is possible due to a dispersive behavior of the effec-

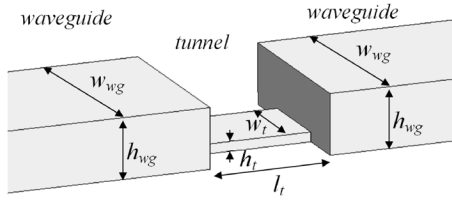


Fig. 1. Layout of an ENZ structure [11].

tive permittivity ϵ_{eff} in a waveguide operated at the TE_{10} mode (1) [11]

$$\frac{\epsilon_{\text{eff}}}{\epsilon_0 \epsilon_r} = n^2 - \frac{c^2}{4\epsilon_r f^2 W_t^2} \quad (2)$$

where n is the refractive index of the substrate material, f is the frequency in operation, and W_t is the waveguide width.

From (2), it is observed that at the cutoff frequency (f_{c10}), $\epsilon_{\text{eff}} = 0$ and the propagation constant is zero ($\beta = 0$), which leads to an infinite phase velocity [11]–[13]. This results in a uniform and strong electric \mathbf{E} -field along the channel [11]–[13].

Fig. 1 shows the layout of a narrow ENZ channel of height h_t and length l_t , connected by two rectangular waveguides of height h_{wg} and width w_{wg} . The three waveguide sections are filled with the same dielectric material with relative real permittivity ϵ_r . If $h_{wg} \gg h_t$, a strong \mathbf{E} -field concentration is observed through the tunnel at the cutoff frequency due to energy squeezing. If an abrupt height difference exists between the feeding waveguides and the tunnel, perfect transmission appears at tunnel cutoff since $\beta = 0$. This super coupling phenomenon associated with the effectively infinite phase velocity of the wave propagation in an ENZ material has some distinct features different from conventional resonance: it is fundamentally independent on the length of the tunnel and its overall geometry. The electromagnetic wave inside the tunnel does not really propagate in an ENZ medium, but rather tunnels through it with an effectively infinite phase velocity. The transmission properties of the channel are simply determined by its input and output ports. The frequency that tunnels through the channel is called tunneling frequency (f_0). This phenomenon can be used for sensing small dielectric variations produced by the insertion of small samples inside the narrow waveguide [11].

In this paper, an ENZ structure at 5.4 GHz is designed using SIW technology [15]. The substrate chosen for the design of the ENZ tunnel structure is RT/Duroid 5880 with permittivity of 2.2 and loss tangent of 0.0009 [18]. The proposed SIW ENZ structure consists of a cavity-tunnel-cavity configuration with dimensions of the tunnel $w_t = 20$ mm, $h_t = 0.5$ mm, and width and length of the cavities of 32 and 10 mm, respectively [14]. SIW cavities are coupled by microstrip transmission lines, as shown in Fig. 2(a). The characteristic impedance of the input/output microstrip is 50Ω . They ensure a complete energy transmission along the whole structure by assigning their SIW TE_{10} dominant mode cutoff frequency below the tunneling frequency. Simulations are performed to realize the SIW ENZ tunnel structure using an electromagnetic wave simulator based on the finite-element method [19]. The dimensions of the tunnel structure shown in Fig. 2(a) are $l_t = 3$ mm, $h_t = 0.5$ mm, $w_t = 20$ mm, $l_{cav} = 10$ mm, $w_{cav} = 32$ mm, $h_{cav} = 3.175$ mm,

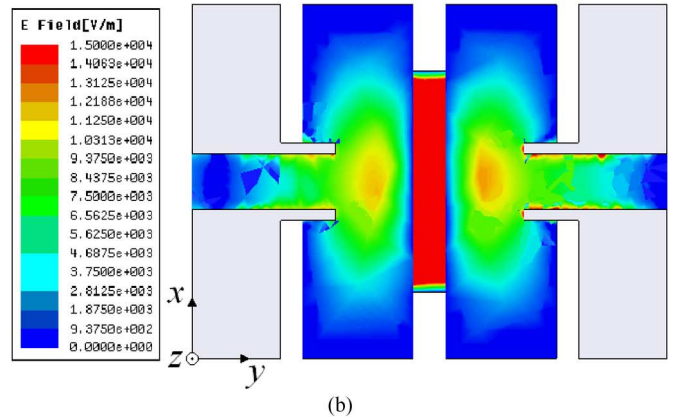
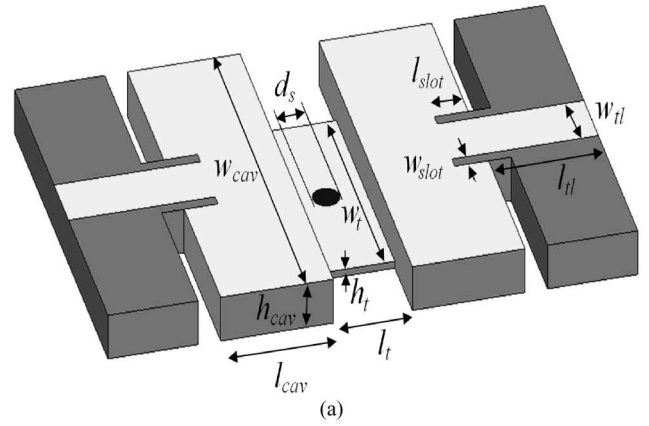


Fig. 2. (a) Proposed SIW ENZ structure. (b) \mathbf{E} -field distribution in the ENZ structure.

$l_{tl} = 10$ mm, $w_{tl} = 5$ mm, $l_{cs} = 3$ mm, $w_{cs} = 1$ mm, and $d_s = 2.4$ mm. The simulated tunneling frequency is $f_0 = 5.36$ GHz. Fig. 2(b) shows the simulated \mathbf{E} -field distribution [19] along the complete structure at the tunneling frequency. It is observed that a strong and constant \mathbf{E} -field enhancement is generated through the narrow tunnel along its y -axis.

B. Tunnel Sensitivity

In order to characterize the permittivity of the samples, a highly sensitive ENZ channel is used. An \mathbf{E} -field enhancement caused by energy squeezing and tunneling in the narrow channel ensures the high sensitivity to small permittivity variations of the samples. The dielectric properties of the sample materials are related to variations in the frequency response of the device. In this paper, dielectric samples of 2.4-mm diameter and 0.5-mm height are placed at the center of the ENZ channel, as shown in Fig. 2(a). Samples of different complex permittivity values are chosen for the analysis. Fig. 3 presents the tunnel frequency response with the insertion of different dielectric samples ($\epsilon'_s = 1, 2, 3$, and 5). It is important to note that the tunneling frequency of the ENZ structure shifts towards higher frequencies (upwards) when the dielectric constant of the sample is less than the dielectric constant of the medium filling the tunnel. The tunneling frequency shifts towards the lower frequencies (downwards) when the dielectric constant of the sample is higher than the dielectric constant of the medium filling the tunnel. This happens due to decrease or increase in

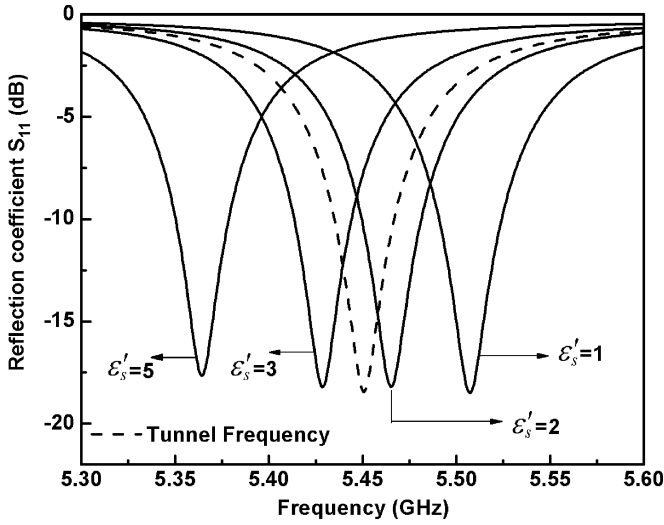


Fig. 3. Variation in tunneling frequency (S_{11}) for different sample dielectric constants.

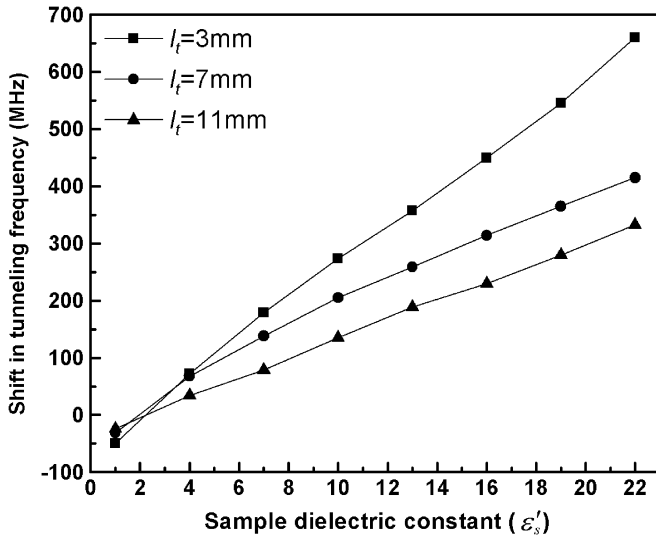


Fig. 4. Shift in tunneling frequency versus sample permittivity coefficient for three different tunnel lengths.

the effective dielectric constant of the tunnel when perturbation of the structure is realized with a sample having dielectric constants different than that of the ENZ medium.

As the tunneling frequency is independent on the length l_t of the ENZ channel due to its quasi-static behavior [11]–[13], a detailed analysis on sensitivity of the ENZ structure is performed by varying the length of the tunnel l_t , and keeping the sample dimensions constant. Simulations are performed for three different tunnel lengths (3, 7, and 11 mm) for various dielectric samples by keeping width and height of the tunnel as 20 and 0.5 mm, respectively. Fig. 4 shows the shift ($f_0 - f_s$) in the simulated tunneling frequency with the real permittivity of several samples for three different tunnel lengths. The reference value f_0 is the tunneling frequency of the structure before perturbation with the sample.

From Fig. 4, it is observed that a shift of 660 MHz is obtained for the sample dielectric permittivity of 22 with the tunnel of length $l_t = 3$ mm. A tunnel with $l_t = 7$ mm presents a variation of 410 MHz for the sample dielectric permittivity of 22, while a tunnel of $l_t = 11$ mm produces a shift of 325 MHz for the same sample permittivity. It is evident that a shorter tunnel length produces higher sensitivity. This can be explained from the cavity perturbation technique (3), (5).

The complex dielectric permittivity values are obtained using cavity perturbation formulae for the SIW resonator expressions. The derivation of the cavity perturbation formulas for the SIW cavity resonators is explained in detail elsewhere [10]. The cavity perturbation expressions for the evaluation of the complex dielectric permittivity are given as follows:

$$\epsilon'_s = \frac{A\epsilon'_r V_c}{V_s} \left(\frac{f_0 - f_s}{f_s} \right) + \epsilon'_r \quad (3)$$

and

$$\epsilon''_s = \frac{BV_c}{V_s} \left(\frac{\epsilon_r'^2 + \epsilon_r''^2}{\epsilon_r'} \right) \left(\frac{Q_0 - Q_s}{Q_0 Q_s} \right) + \frac{\epsilon_s' \epsilon_r''}{\epsilon_r'} \quad (4)$$

where ϵ'_s and ϵ''_s are the real and imaginary permittivities of the sample, respectively, ϵ'_r is the substrate relative permittivity, and ϵ_r'' is related to the substrate loss tangent as $\epsilon_r'' = \epsilon'_r \tan \delta$; f_0 and f_s are the tunneling frequencies before and after the small perturbation, respectively. Q_0 and Q_s are the quality factors of the tunnel before and after perturbation with the sample. V_c and V_s correspond to volume of the tunnel and volume of the sample, respectively. A and B are related to the structure configuration, mode of operation of the structure, and shape and position of the sample inside the tunnel. As it is difficult to obtain A and B analytically, these parameters are obtained experimentally by using standard samples of known dielectric properties [3], [7], [10]. By rearranging (3) into (5) as follows, it becomes evident that for shorter tunnels (smaller V_c), there are larger variations in f_s :

$$\frac{f_0}{f_s} = \frac{V_s}{V_c} \left(\frac{\epsilon'_s - \epsilon'_r}{A\epsilon_r'} \right) + 1. \quad (5)$$

C. Fabrication of the SIW ENZ Structure

To demonstrate the sample dielectric sensing, the ENZ SIW structure is fabricated using a conventional printed circuit board (PCB) milling machine. The proposed structure is implemented on a 3.175-mm-thick RT/Duroid 5880 substrate with relative dielectric constant 2.2 and dielectric loss tangent 0.0009 [18]. The height of the ENZ channel is $h_t = 0.5$ mm. The length of the channel is chosen as $l_t = 3$ mm since it offers the highest sensitivity. All the layers were properly metallized. The dimensions of the optimized tunnel structure, shown in Fig. 5, are $l_t = 3$ mm, $h_t = 0.5$ mm, $w_t = 20$ mm, $l_{cav} = 10$ mm, $w_{cav} = 32$ mm, $h_{cav} = 3.175$ mm, $l_{tl} = 10$ mm, $w_{tl} = 5$ mm, $l_{cs} = 3$ mm, $w_{cs} = 1$ mm, and $d_s = 2.4$ mm. A photograph of the fabricated ENZ tunneling structure is shown in Fig. 5. A 2.4-mm-diameter hole at the center of the ENZ channel is chosen for placing the sample. All the samples are shaped as 2.4-mm-diameter rods to completely fill the hole. The interaction between microwaves and the sample occurs mainly inside

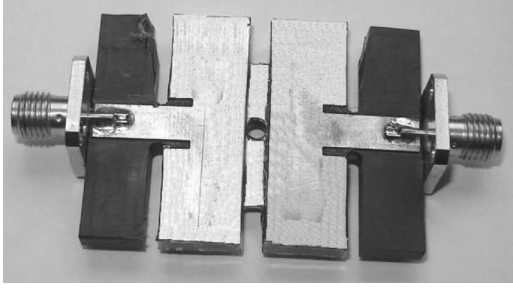


Fig. 5. Photograph of the fabricated ENZ tunnel structure.

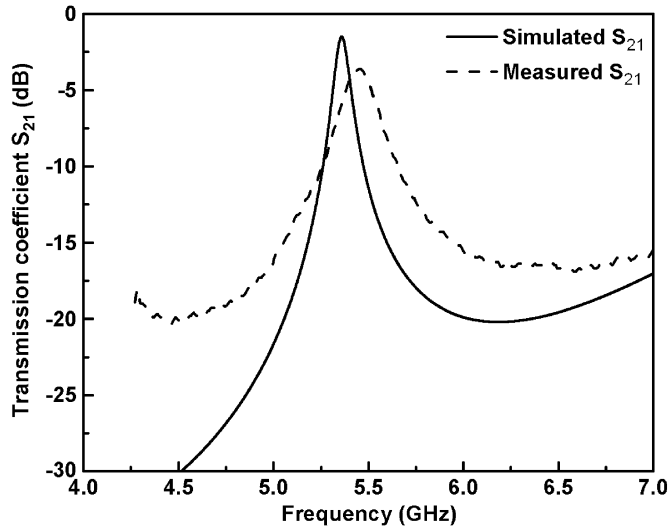


Fig. 6. Simulated and experimental frequency responses of the proposed tunnel structure.

the volume of the tunnel so the height of each sample can be larger than that of the tunnel for mechanical holding.

Measurements are performed using an Agilent PNA-series vector network analyzer (E8361A). Fig. 6 shows the simulated and measured transmission coefficients of the proposed structure. Due to the symmetry of the circuit, calculation of the unloaded Q factor (Q_u) from S_{21} measurements can be determined by using

$$Q_u = \frac{Q_l}{1 - S_{21}(f_0)} \quad (6)$$

where Q_l is the loaded Q factor of the structure and $S_{21}(f_0)$ is the insertion loss magnitude at the tunneling frequency

$$S_{21}(f_0) = 10^{\frac{\alpha}{20}} \quad (7)$$

where α is the insertion loss value in decibels.

The simulated and measured tunnel frequencies and unloaded Q factors (Q_u) of the proposed structure are 5.359 and 5.5018 GHz and 397 and 155.15, respectively. Results demonstrate that the fabricated structure has a shift in the desired frequency around 142 MHz. Discrepancy in the Q_u factors are mainly due to manufacturing errors and the additional connector losses. Simulated and measured insertion losses at f_0 are 1.5 and 2.75 dB, respectively. The difference between simulation and measurement results may be caused by the manufacturing and material tolerances to some degree.

TABLE I
DIELECTRIC CHARACTERISTICS OF STANDARD SAMPLES
AND CALIBRATION CONSTANTS

Sample	f_s (GHz)	ϵ'	Q_u	ϵ''	A	B
Teflon	5.5034	2.1	154.86	0.0021	11.78	0.62
RO4003	5.4836	3.38	149.21	0.0091	12.16	0.81
duroid 6010.2	5.3782	10.2	144.06	0.0235	11.93	0.88

III. MATERIAL CHARACTERIZATION

The samples used in this study are standard materials: Teflon [16], RT/Duroid 5880 [18], Acrylic, Nylon, Rogers RO4003 [18], wood, quartz [17], Rogers RT/Duroid 6010.2LM [18], and RT/Duroid 6010.8LM [18]. The fabricated ENZ tunnel structure is connected to the ports of the PNA-series microwave vector network analyzer. A hole has been manufactured at the center of the tunnel where the maximum electric \mathbf{E} -field occurs. The samples are inserted into the ENZ structure and the shift in the tunneling frequency (f_s) and quality factor (Q_{us}) are analyzed from S_{21} -parameters of the network analyzer. The measurements were repeated four times and the data was averaged. Sample dielectric constant and dielectric loss values are obtained from the shift in the tunnel frequency and change in the Q_u factor, respectively, using the cavity perturbation technique [10].

Standard samples of known permittivity characteristics (Teflon [16], Rogers RO4003 [18], and Rogers RT/Duroid 6010.2LM [18]) are used to evaluate the calibration constants A and B , which are obtained from the shift in the tunneling frequency and the change in the Q_u factor of the tunnel structure for each sample. The dielectric characteristics of the Rogers substrates are obtained at 5.5 GHz from the datasheets [18]. Table I shows the average values of the tunneling frequencies, Q_u factors, dielectric constants, and calibration constant for each of the standard samples.

The small differences of A and B parameters in Table I for each of the standard materials are due to manufacturing tolerances of the prepared samples. For the material characterization, the average of A and B calibration values (11.96 and 0.77, respectively) are used in the perturbation technique. Fig. 7 shows the measured tunneling frequency versus real permittivity of the measured samples. Table II compares the experimental and literature [18] values of the samples. It is clearly observed that good agreement between reported and measured data is obtained. The error in the measured values of ϵ'_s in comparison with the standard materials using the ENZ structure is within 3%. The measured ϵ''_s error for the different samples falls within 13% of the literature values. The higher discrepancies between the literature and measured ϵ'' values are mainly due to the addition of connector losses in the Q_u calculations.

IV. SENSITIVITY ANALYSIS

Sensitivity analyses for the ENZ tunnel structure and SIW cavity resonator are performed. Fig. 8 shows the layout of the ENZ tunnel structure and SIW resonant cavity. A detailed explanation of the SIW cavity resonator chosen for analysis is mentioned elsewhere [10]. A TE_{103} SIW cavity resonating at 5 GHz is designed using an RT/Duroid 5880 substrate ($\epsilon'_r = 2.2$, $\tan \delta = 0.0009$, and thickness $h = 3.175$ mm [18]) based

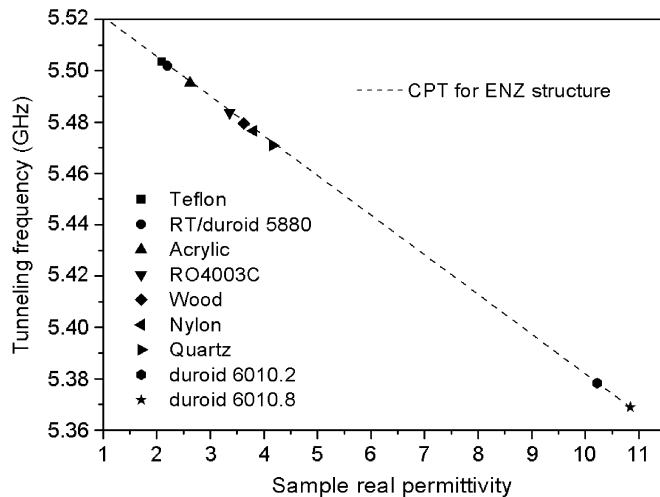


Fig. 7. Measured tunneling frequency versus dielectric constant of standard materials, and CPT characterization.

TABLE II
COMPARISON BETWEEN REPORTED AND MEASURED VALUES
OF SAMPLE DIELECTRIC CONSTANTS

Material	f_0 (GHz)	REPORT ϵ'_s	MEAS ϵ'_s	Q_u	REPORT ϵ''_s	MEAS ϵ''_s
RT/dur. 5880	5.502	2.2	2.200	155.1	0.0019	0.0019
Acrylic	5.495	2.7	2.623	144.9	-	0.0125
Wood	5.479	-	3.625	117.9	-	0.0491
Nylon	5.477	-	3.809	136.7	-	0.0229
Quartz	5.471	4.2	4.167	155.7	-	0.0032
6010.8	5.369	10.8	10.837	143.2	0.0248	0.0218

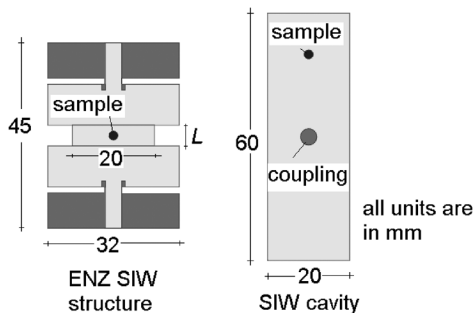


Fig. 8. Schematics of the ENZ SIW structure and SIW cavity resonator.

on the SIW design criteria [10], [15]. The dimensions of the cavity are $a = 20$ mm and $d = 60$ mm. The walls of the SIW cavity are completely metallized. Probe coupling is chosen for the excitation of the cavity.

Full-wave simulations [19] are carried out with different dielectric permittivity values using these ENZ tunnel structure and the SIW cavity resonator. Samples of different dielectric permittivity values, ranging from $\epsilon'_s = 1$ –22, have been chosen for characterization.

Fig. 9 shows the shift in the tunneling frequency and resonant frequency versus sample dielectric permittivities with ENZ

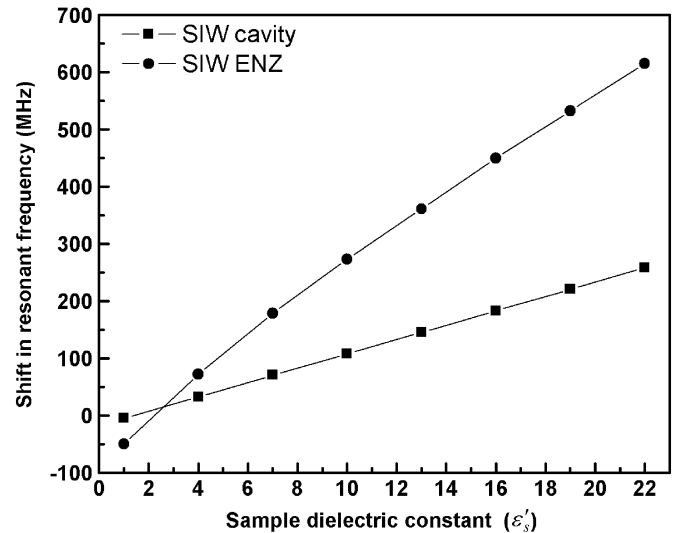


Fig. 9. Shift in tunneling frequency versus sample permittivity for the ENZ structure and SIW cavity resonator.

tunnel and SIW cavity resonator, respectively. It is clear that the shift in resonant/tunneling frequency increases with the increase in the dielectric constant of material for both structures. It can be observed from Fig. 9 that a change in the sample dielectric permittivity of 0.5 generates a shift of 6.3 MHz in the resonant frequency for the SIW cavity resonator, whereas for the ENZ tunnel structure, the shift in the tunneling frequency is about 17 MHz.

The sensitivity $s = dF/d\epsilon'_s$ [with fractional change in the resonant/tunneling frequency $F = (f_0 - f_s)/f_s$] of the SIW cavity resonator obtained from simulations is 0.2%, while the sensitivity for the ENZ tunnel structure is of 0.7%. It is evident that the ENZ tunnel yields better sensitivity when compared to SIW cavity resonators. This enhanced sensitivity is due to the dramatic field concentration caused by energy squeezing in ultra narrow waveguide channels with near-zero effective permittivity. This high sensitivity will help to sense small permittivity variations of the materials.

V. CONCLUSION

A compact high-sensitivity SIW ENZ structure has been presented for the evaluation of complex dielectric permittivity of materials. Simulations and measurements are performed on various dielectric samples using cavity perturbation technique for the proposed structure. The evaluated values of complex permittivity are in good agreement with the theoretical values. Errors in the measured values of the dielectric constant and dielectric loss are within 3% and 13%, respectively. Moreover, sensitivity analyses have been performed on the SIW ENZ structure and conventional SIW cavities. The proposed structure presents higher sensitivity and compact size when compared to conventional SIW cavities.

REFERENCES

- [1] W. H. Surber, Jr., "Universal curves for dielectric-filled wave guides and microwave dielectric measurements method for liquids," *J. Appl. Phys.*, vol. 19, no. 6, pp. 514–523, Jul. 1948.

- [2] M. Jeyaraj, A. Kumarasamy, and J. Sobhanadri, "Numerical curve fitting technique for evaluating complex permittivity of liquids of millimetre and centimetre wavelengths," *J. Phys. E, Sci. Instrum.*, vol. 12, no. 12, pp. 1179–1183, Dec. 1979.
- [3] T. W. Dakin and C. N. Works, "Microwave dielectric measurements," *J. Appl. Phys.*, vol. 18, no. 9, pp. 789–797, Sep. 1947.
- [4] H. K. Henisch and J. Zucker, "Contactless method for the estimation of resistivity and lifetime of semiconductors," *Rev. Sci. Instrum.*, vol. 27, no. 6, pp. 409–410, Jun. 1956.
- [5] E. Nyfors, "Industrial microwave sensors—A review," *Subsurf. Sens. Tech. Apps.*, vol. 1, no. 1, pp. 23–43, Jan. 2000.
- [6] P. A. Bernard and J. M. Gautray, "Measurement of dielectric constant using microstrip ring resonator," *IEEE Trans. Microw. Theory Tech.*, vol. 39, no. 3, pp. 592–595, Mar. 1991.
- [7] K. Saeed, R. D. Pollard, and I. C. Hunter, "Substrate integrated waveguide cavity resonator for complex permittivity characterization of materials," *IEEE Trans. Microw. Theory Tech.*, vol. 56, no. 10, pp. 2340–2347, Oct. 2008.
- [8] T. Sokoll and A. F. Jacob, "Self-calibration circuits and routines for low-cost measuring systems," *Microw. Opt Technol. Lett.*, vol. 50, no. 2, pp. 287–293, Feb. 2008.
- [9] D. M. Pozar, *Microwave Engineering*, 3rd ed. New York: Wiley, 2005.
- [10] H. Lobato-Morales, A. Corona-Chávez, D. V. B. Murthy, and J. L. Olvera-Cervantes, "Complex permittivity measurements using cavity perturbation technique with substrate integrated waveguide cavities," *Rev. Sci. Instrum.*, vol. 81, no. 6, pp. 064704-1–064704-4, Jun. 2010.
- [11] A. Alu and N. Engheta, "Dielectric sensing in ϵ -near-zero narrow waveguide channels," *Phys. Rev. B, Condens. Matter*, vol. 78, no. 4, pp. 45102-1–45102-5, Jul. 2008.
- [12] W. Rotman, "Plasma simulation by artificial dielectrics and parallel-plate media," *IRE Trans. Antennas Propag.*, vol. 10, no. 1, pp. 82–95, Jan. 1962.
- [13] B. Edwards, A. Alu, M. E. Young, M. Silveirinha, and N. Engheta, "Experimental verification of epsilon-near-zero metamaterial coupling and energy squeezing using a microwave waveguide," *Phys. Rev. Lett.*, vol. 100, no. 3, pp. 033903-1–033903-4, Jan. 2008.
- [14] H. Lobato-Morales, A. Corona-Chávez, D. V. B. Murthy, J. Martínez-Brito, and L. G. Guerrero-Ojeda, "Experimental dielectric sensing of materials using epsilon-near-zero tunnel in SIW technology," in *IEEE MTT-S Int. Microw. Symp. Dig.*, 2010, pp. 1644–1647.
- [15] M. Bozzi, F. Xu, D. Deslandes, and K. Wu, "Modeling and design considerations for substrate integrated waveguide circuits and components," in *Int. Telecomm. Modern Satellite, Cable, Broadcast. Serv. Conf.*, Sep. 2007, pp. 7–16.
- [16] V. Subramanian, V. Sivasubramanian, V. R. K. Murthy, and J. Sobhanadri, "Measurement of complex dielectric permittivity of partially inserted samples in a cavity perturbation technique," *Rev. Sci. Instrum.*, vol. 67, no. 1, pp. 279–282, Jan. 1996.
- [17] J. Baker-Jarvis, R. G. Geuer, J. H. Grosvenor, Jr., M. D. Janezic, C. A. Jones, B. Riddle, and C. M. Weil, "Dielectric characterization of low-loss materials: A comparison of techniques," *IEEE Trans. Dielectr. Electr. Insul.*, vol. 5, no. 4, pp. 571–577, Aug. 1998.
- [18] "High frequency laminates," Rogers Corporation, Rogers, CT, Datasheet, 2010.
- [19] High Frequency Structure Simulator (HFSS). ver. 10, Ansoft Corporation, Pittsburgh, PA, 2005.



Humberto Lobato-Morales (S'05) received the B.Sc. and M.Sc. degrees from Universidad de las Américas-Puebla (UDLA-P), Cholula, Puebla, México, in 2006 and 2008, respectively, and is currently working toward the Ph.D. in electronics engineering at the Instituto Nacional de Astrofísica, Óptica y Electrónica (INAOE), Tonantzintla, Puebla, México.

In 2008, he joined the Emerging Microwave Technologies Group (EMT), INAOE, as a Research Engineer. His research interests include microwave filters

and multiplexers, microwave metamaterials, and material characterization using microwaves.



D. V. B. Murthy received the B.Sc. degree from Andhra University, Andhra Pradesh, the B.Eng. degree from the Institute of Engineers, Kolkata, India, the M.Sc. degree from Madras University, Chepauk, Chennai, India, and the Ph.D. degree in microwave physics from the Indian Institute of Technology, Madras, India, in 2007.

In 2007, he joined the Instituto Nacional de Astrofísica, Óptica y Electrónica (INAOE), Tonantzintla, Puebla, México, as an Associate Researcher. His current research interests include metamaterials,

SIW circuits, passive millimeter-wave imaging, ultra-wideband (UWB) antennas, microwave measurements on semiconductors, heterostructures, and polymer-carbon nanotubes.



Alonso Corona-Chávez (S'00–A'01–M'02–SM'09) received the B.Sc. degree from the Tecnológico de Monterrey (ITESM), México, in 1997, and the Ph.D. degree from the University of Birmingham, Edgbaston, Birmingham, U.K., in 2001.

From 2001 to 2004, he was a Microwave Engineer with Cryosystems Ltd. During this time, he was also an Honorary Research Fellow with the School of Electrical Engineering, University of Birmingham. In 2004, he joined the Instituto Nacional de Astrofísica, Óptica y Electrónica (INAOE), Tonantzintla, Puebla,

México, where he is currently a Professor of electronics. He is the Head of the Emerging Microwave Technologies Group (EMT), INAOE. His current interests include microwave applications of HTS, RF, and microwave devices for communications and radio astronomy.

Prof. Corona-Chávez was the recipient of a Fulbright Fellowship to carry out research with the Electrical Engineering Department, University of California at Los Angeles (UCLA) in April 2009.



José Luis Olvera-Cervantes received the B.Sc. degree from the Instituto Politécnico Nacional (IPN), México, in 2001, and the M.Sc. and Ph.D. degrees from the Centro de Investigación Científica y de Educación Superior de Ensenada (CICESE), México, in 2005 and 2008, respectively.

He then joined the Georgia Institute of Technology, Atlanta, and the Georgia Electronic Design Center (GEDC), Atlanta. In 2009, he joined the Instituto Nacional de Astrofísica, Óptica y Electrónica (INAOE), Tonantzintla, Puebla, México. His research is focused

on characterization of microwave transistors at room and cryogenic temperatures, low-noise amplifiers, microwave filters, and planar antennas.

Juan Martínez-Brito received the B.Sc. degree from the Universidad de las Américas-Puebla (UDLA-P), Cholula, Puebla, México, in 2010.

He was collaborating with the Emerging Microwave Technologies Group (EMT), Instituto Nacional de Astrofísica, Óptica y Electrónica (INAOE), Tonantzintla, Puebla, México, in the research of measurement of materials using microwave techniques.

Luis Gerardo Guerrero-Ojeda (M'02) received the B.Sc. and M.Sc. degrees from the Universidad de las Américas-Puebla (UDLA-P), Cholula, Puebla, México, in 1990 and 1994, respectively.

In 1997, he joined UDLA-P as a Professor with the Electronics Engineering Department. His areas of interest include telecommunication systems, RF, and EM theory.